

Dynamic correlated Cu(2) magnetic moments in superconducting $\text{YBa}_2(\text{Cu}_{0.96}\text{Ni}_{0.04})_3\text{O}_y$ ($y \sim 7$)

J.A. Hodges, P. Bonville, A. Forget
CEA, Centre d'Etudes de Saclay,
DSM/IRAMIS/Service de Physique de l'Etat Condensé,
91191 Gif-sur-Yvette, France

A. Yaouanc, P. Dalmas de Réotier
CEA/DSM/Institut Nanosciences et Cryogénie, 38054 Grenoble, France

S.P. Cottrell
ISIS Facility, Rutherford Appleton Laboratory, Chilton, Didcot, OX11 0QX, UK

We have examined the magnetic properties of polycrystalline, superconducting $\text{YBa}_2(\text{Cu}_{0.96}\text{Ni}_{0.04})_3\text{O}_y$ ($y \sim 7$, $T_{\text{sc}} \sim 75$ K) using two local probe techniques: ^{170}Yb Mössbauer down to 0.1 K and muon spin relaxation (μSR) down to 1.5 K. At 0.1 K, the ^{170}Yb measurements show the Cu(2) over essentially all the sample volume carry magnetically correlated moments which are static on the time-scale 10^{-9} s. The moments show a distribution in size. The correlations are probably short range. As the temperature increases, the correlated moments are observed to fluctuate with measurable rates (in the GHz range) which increase as the temperature increases and which show a wide distribution. The μSR measurements also evidence that the fluctuation rates increase with increasing temperature and there is a distribution. The evidenced fluctuating, correlated Cu(2) moments coexist at an atomic level with superconductivity.

PACS numbers: 74.72.Bk, 74.25.Ha, 76.80.+y, 76.75.+i

I. INTRODUCTION

Superconductivity occurs in the cuprates when a sufficient density of carriers is introduced into the Cu-O planes of the parent compound which is essentially an antiferromagnetic insulator. This feature has stimulated much work directed towards understanding the link between magnetism and superconductivity in these compounds. Two particular centres of interest concern a), the possible role of spin fluctuations in mediating superconductivity and b), the antiferromagnetism - superconductivity phase diagram as a function of carrier density. This latter aspect also embraces the question whether or not antiferromagnetic order and superconductivity are always mutually exclusive on an atomic level.

In $\text{YBa}_2\text{Cu}_3\text{O}_y$, the Cu occupy Cu(1) (chain) and Cu(2) (plane) sites. The phase diagram extends from $y \simeq 6$, where the compound is a Mott insulator and the Cu(2) of the planes order antiferromagnetically to $y \simeq 7$, where it is an optimally doped superconductor ($T_{\text{sc}} \sim 90$ K) and the Cu(2) do not carry magnetic moments. The introduction of a low level of doping into the insulator leads to the breakdown of the long range order and the introduction of dynamical features. Some Cu(2) based magnetic order persists in samples with intermediate doping levels which show superconductivity¹. Moments linked with orbital currents have also been evidenced² but not confirmed³. In the intermediate doping region, early theoretical studies based on the Hubbard and t-J models, envisaged segregation into charge poor (antiferromagnetic Cu(2)) and

charge rich (superconducting) regions^{4,5,6}, in which case the observed Cu(2) magnetic order would involve only part of the sample. Although local probe measurements on underdoped polycrystalline samples evidence segregation into magnetic and non-magnetic regions⁷, it is problematic, in such samples, to experimentally determine whether or not superconductivity and Cu(2) magnetic order are mutually exclusive at an atomic level.

The question may thus be asked, are there cases in the cuprates where the carrier density is high enough for well developed superconductivity to exist but where the Cu(2) remain magnetically ordered? This is clearly not an omnipresent possibility as shown by the discussions concerning the existence of a quantum critical point⁸, but it is still of interest to examine whether Cu(2) magnetic order and superconductivity can coexist at an atomic level in specific cases.

Here we show that in absence of any applied magnetic field, all the Cu(2) in fully oxidized, superconducting $\text{YBa}_2(\text{Cu}_{0.96}\text{Ni}_{0.04})_3\text{O}_y$ ($y \sim 7$) carry correlated magnetic moments. The correlations are probably short-range. Nuclear Magnetic Resonance (NMR) results on equivalent samples have previously shown that field induced staggered Cu(2) magnetic moments are nucleated around the substituted Ni both above⁹ and below¹⁰ T_{sc} .

II. SAMPLES, METHODOLOGY

For the Mössbauer measurements, a single phase polycrystalline sample of $\text{Y}_{0.975}\text{Yb}_{0.025}\text{Ba}_2(\text{Cu}_{0.96}\text{Ni}_{0.04})_3\text{O}_y$ ($y \sim 7$) was prepared through conventional cycles of sin-

tering and crushing, followed by oxygen anneals. The Yb was enriched in the Mössbauer isotope ^{170}Yb . We recall that the Yb^{3+} ion is a non-perturbing probe in that it has no influence on the superconductivity (neither on T_{sc} nor on the Meissner fraction) and it has no influence on any Cu(2) based magnetic order. The total signal provided by a Mössbauer measurement contains contributions coming from each and every individual ^{170}Yb probe in the sample. The measurements thus provide information which concerns the total sample volume.

An equivalent single phase sample which did not contain any Yb was prepared in the same way for the μSR measurements. DC susceptibility measurements, made down to 4.2 K, provided the T_{sc} values of ~ 75 K (with or without Yb) which is a typical value for a Ni concentration of 4 %. These measurements also showed that as the temperature is reduced, the (negative) Meissner susceptibility is essentially independent of temperature below ~ 50 K.

The Mössbauer measurements on the paramagnetic $^{170}\text{Yb}^{3+}$ probes were carried out in absence of any applied field. We recall the main aspects^{7,11,12}. The $^{170}\text{Yb}^{3+}$ probes, which substitute at the Y^{3+} site within the Cu(2) - O bilayers, are randomly distributed throughout the sample volume. The average in-plane distance between two probes is ~ 5 a or b lattice parameters. The majority of the $^{170}\text{Yb}^{3+}$ thus behave as isolated probes in that they have no interaction with any other of the Yb^{3+} . In principle, there will be a spin-spin interaction linking the small fraction of the Yb^{3+} which have a Ni as a near neighbour but experimentally this interaction plays a negligible role. The only interaction that is clearly detected by the $^{170}\text{Yb}^{3+}$ is the molecular field which acts on its spin. This field is present when the nearest neighbour Cu(2) to a Yb^{3+} carry correlated magnetic moments. These magnetically correlated Cu(2) are initially nucleated around each Ni. If we observe that all (or a fraction) of the probes experience a molecular field, this shows the Cu(2) in all (or in a fraction) of the sample carry magnetic moments that are correlated. This local probe technique provides no information concerning the size of the Cu(2) moments nor their magnetic correlation length. However, it provides information concerning the fluctuation rate of the molecular field (the fluctuation rate of the correlated Cu(2) magnetic moments) provided this falls within the ^{170}Yb Mössbauer frequency window for which the lower bound is $\sim 10^9 \text{ s}^{-1}$.

An introduction to the positive muon spin rotation/relaxation (μSR) techniques is given in Refs. 13,14. The measurements were carried out at the MuSR spectrometer of the ISIS facility, Rutherford-Appleton Laboratory, Chilton, UK.

Both the substituted $^{170}\text{Yb}^{3+}$ probes and the implanted muon probes furnish information concerning the local magnetic properties of the matrix by detecting the internal fields that are produced on them. For the $^{170}\text{Yb}^{3+}$ probe, it is a molecular field that is detected, whereas for the muon probe, it is the longer range dipolar

field. The two techniques thus examine the local magnetic properties over somewhat different length scales. Both techniques can also provide information concerning the fluctuation rates of the field.

III. EXPERIMENTAL RESULTS

A. ^{170}Yb Mössbauer probe data and analysis

The ^{170}Yb Mössbauer measurements ($I_g = 0$, $I_{ex} = 2$, $E_\gamma = 84 \text{ keV}$, $1 \text{ mm/s} = 68 \text{ MHz}$) were made using a source of Tm^*B_{12} and a linear velocity sweep.

The analysis of the experimental lineshapes to be presented below, is made in terms of the electro-nuclear (Breit-Rabi) Hamiltonian comprising a hyperfine interaction and an electronic Zeeman term :

$$\mathcal{H} = S' \cdot \mathbf{A} \cdot \mathbf{I} + \mu_B S' \cdot \mathbf{g} \cdot \mathbf{H}(t). \quad (1)$$

\mathbf{A} and \mathbf{g} are the known hyperfine and g-tensors associated with the Yb^{3+} ground state Kramers doublet¹², μ_B is the Bohr magneton and $\mathbf{H}(t)$ the fluctuating molecular field acting on the Yb^{3+} which has an effective spin $S'=1/2$. The energy equivalent of each of the two terms is of order 0.1 K.

We first show on Fig.1 simulated lineshapes corresponding to Eq. 1 for different fluctuation rates of the molecular field. The three different lineshapes correspond to the three types of (sub)spectra that are encountered experimentally. The field intensity is fixed at the value 0.2 T. The top lineshape (multicomponent lineshape) was calculated from Eq. 1 with the field “static” on the ^{170}Yb Mössbauer frequency scale, *i.e* if the field fluctuates, it does so at a rate which is below the lower limit of the Mössbauer frequency window ($\sim 10^9 \text{ s}^{-1}$). The middle lineshape (single component lineshape) was obtained with the field fluctuating within the frequency window at a rate $5 \times 10^{10} \text{ s}^{-1}$ and the bottom lineshape (doublet lineshape) was calculated with the field fluctuating above the frequency window (fluctuating too fast to be detected). This lineshape also corresponds to the case when the field is simply absent. Experimentally, the assessment as to whether, at a particular temperature, the field has no influence on the lineshape because it fluctuates too fast or because it is absent, has to be made by examining the thermal dependence of the field in the temperature range where it is visible.

Experimental data were obtained over the range 0.1 to 70 K and data for three selected temperatures are shown on Fig.2. We first note that although only one type of sub-spectrum (the multicomponent lineshape but with two slightly different forms) is present at 0.1 K, at higher temperatures quite different subspectra are simultaneously present. For example, on Fig.2 at 2.5 K, the three subspectra corresponding to the three examples on Fig.1 are all present with different relative weights. Our local probe technique thus shows that at specific temperatures,

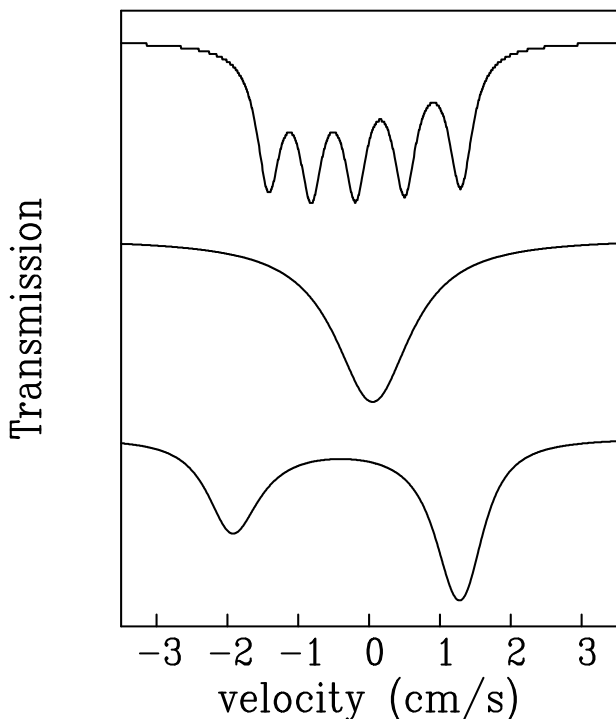


FIG. 1: Calculated ^{170}Yb Mössbauer absorption spectra corresponding to Hamiltonian (1) for a field $H(t)$ of 0.2 T fluctuating at rates below (top), within (middle) and above (bottom) the accessible frequency window. See the text for details. These calculated spectra correspond to the forms of the (sub)spectra evidenced experimentally in Fig.2.

it is possible to identify the coexistence of quite different local behaviours. The same situation was also evidenced in $\text{YBa}_2(\text{Cu}_{1-x}\text{Co}_x)_3\text{O}_7^{11}$.

At 0.1 K, only the multicomponent lineshape shown at the top of Fig.1 is present. This indicates that each of the Yb^{3+} spins throughout the sample experiences a molecular field which is static on the time scale 10^{-9}s . The presence of this field on all of the probes indicates that essentially all the Cu(2) of the sample carry magnetic moments which are at least short range correlated and which appear static. The best data fit is obtained with a molecular field that shows a distribution in size. The effect of the distribution is well mimicked by fitting in terms of two fields (0.22 T on 62% of the probes and 0.07 T on 38%) (Fig.2 top). The weighted mean provides the average field (0.16 T) and the difference between the two fields (0.15 T) provides an estimate of the range of the distribution. Our observation of a distribution in the size of the molecular field suggests there is a distribution in the size of the correlated Cu(2) magnetic moments. ^{17}O NMR measurements on analogous Ni substituted samples (Sec. IV) have evidenced that the size of the staggered Cu(2) magnetic moments observed in an applied magnetic field depend on the distance between a Cu(2) and a Ni. Our results evidence that correlated Cu(2) moments exist in absence of an applied field and they show

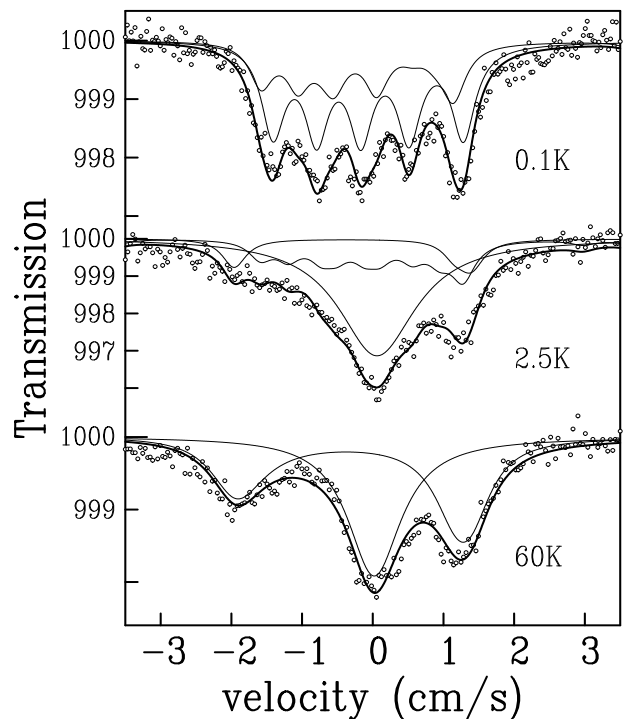


FIG. 2: ^{170}Yb Mössbauer absorption spectra for $\text{Y}_{0.975}\text{Yb}_{0.025}\text{Ba}_2(\text{Cu}_{0.96}\text{Ni}_{0.04})_3\text{O}_y$ ($y \sim 7$). Different subspectra are present and the line fits are explained in the text.

an intrinsic distribution in size. The average size of the molecular field obtained here is similar to that observed on Yb^{3+} in superconducting $\text{YBa}_2(\text{Cu}_{0.96}\text{Co}_{0.04})_3\text{O}_7^{11}$, where the Cu(2) moments which give rise to the field have an average value of a fraction of a μ_B ¹⁵. We thus suggest the average size of the correlated Cu(2) moments in the present Ni substituted samples is of the order of a fraction of a μ_B . We have no direct information concerning the directional properties of the correlated Cu(2) magnetic moments. However, since we find the average size and the average direction of the molecular field observed here are similar to those observed on the ^{170}Yb probe in other cuprates where the Cu(2) moments lie in the (ab) plane^{11,15}, it is possible that here also, the Cu(2) magnetic moments also lie towards the (ab) plane.

The variation of the line shapes as a function of increasing temperature follows roughly the same evolution observed in $\text{YBa}_2(\text{Cu}_{0.96}\text{Co}_{0.04})_3\text{O}_y$ ($y \sim 7$)¹¹ but the changes take place at much lower temperatures in the sample substituted with Ni than in the sample substituted with Co. In $\text{YBa}_2(\text{Cu}_{0.96}\text{Ni}_{0.04})_3\text{O}_7$ there is a relatively rapid change up to $\sim 3.0\text{K}$: at 2.5 K (Fig.2), a “static” molecular field (multicomponent subspectrum) is now present on only $\sim 30\%$ of the Yb^{3+} ions and no field (doublet subspectrum) is visible on $\sim 12\%$ of the Yb^{3+} with the remainder corresponding to the singlet component lineshape. Above $\sim 3.0\text{K}$, the subspectrum corresponding to a “static” field is no longer visible and

there is a progressive change in the relative weights of the two remaining subspectra. Fig.2 shows that at 60 K, the relative weight of the subspectrum corresponding to no visible field (doublet subspectrum) has increased to $\sim 50\%$. The analysis of the lineshapes at the different temperatures evidences a) at each particular temperature there is a wide distribution in the local fluctuation rates and b) the average fluctuation rate increases as the temperature is increased. Because of the wide distribution in the rates, it is difficult to obtain accurate values for the average rates. We simply estimate that on increasing the temperature to 60 K, this average rate increases progressively by two to three orders of magnitude above the threshold value of 10^9 s^{-1} .

If the evolution in $\text{YBa}_2(\text{Cu}_{0.96}\text{Ni}_{0.04})_3\text{O}_7$ is considered as a function of decreasing temperature, the fluctuation rates decrease progressively. It thus seems likely that the correlated moments continue to fluctuate at 0.1 K and below, but with rates that are below 10^9 s^{-1} and thus too low to be experimentally accessible using ^{170}Yb .

B. μSR probe data and analysis

μSR measurements have been carried out on $\text{YBa}_2(\text{Cu}_{1-x}\text{Ni}_x)_3\text{O}_y$ by Bucci *et al.*¹⁶ with the aim of examining the influence of the Ni on the magnetic penetration depth. The measurements were made down to 35 K and did not incidentally evidence the influence of the magnetic fluctuations on the asymmetry. As shown below, this influence is only visible well below 35 K.

Our μSR measurements were carried out from 100 K to 1.5 K in zero applied field and at 1.5 K in longitudinal fields (applied in the field cooled configuration) up to 200 mT. In zero applied field, the measured asymmetry, *i.e.* the μSR signal, is essentially independent of temperature from 100 to ~ 5 K and it then changes progressively as the temperature is further lowered (Fig. 3).

The measured spectra are expressed as the product of a_0 , the effective asymmetry of the muon decay, and $P_Z^{\text{exp}}(t)$, the polarisation function of interest¹³. $a_0 P_Z^{\text{exp}}(t)$ is a sum of two components: the first originating from the sample and the second from the sample holder and surroundings. We write

$$a_0 P_Z^{\text{exp}}(t) = a_s P_Z^s(t) + a_{\text{bg}}, \quad (2)$$

where $a_{\text{bg}} = 0.099$.

From 100 to ~ 5 K, the asymmetry is nicely modelled by the Kubo-Toyabe function, *i.e.* $P_Z^s(t) = P_Z^{\text{KT}}(t)$, linked with the interaction between the nuclear magnetic moments and the muon spin. We find $a_s = 0.153(1)$ and for the field width at the muon site $\Delta^{KT} = 0.146(2)$ mT. This Δ^{KT} value is close to that for unsubstituted $\text{YBa}_2\text{Cu}_3\text{O}_7$ ¹⁷.

As the temperature is lowered below ~ 5 K, the time dependence of the asymmetry becomes progressively more rapid. This behaviour is due to the influence of

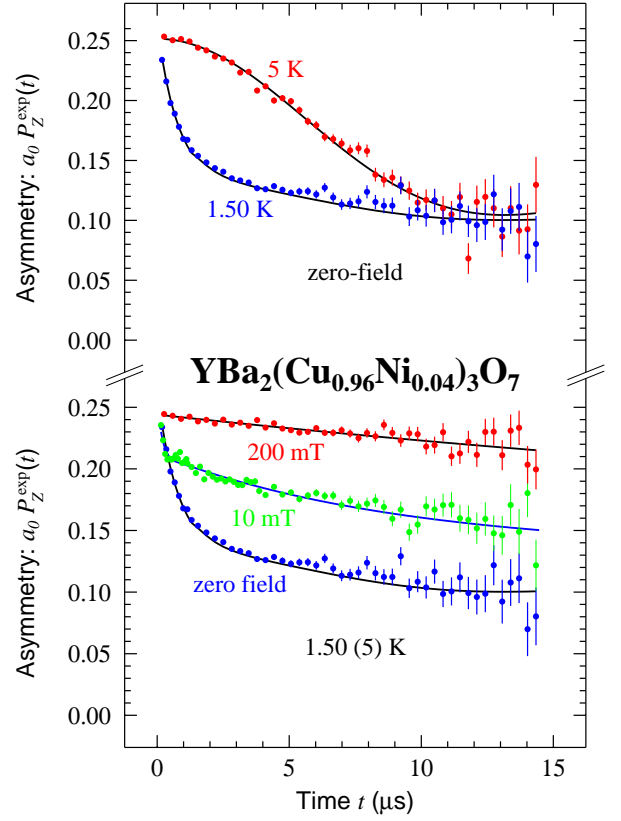


FIG. 3: (color online). Examples of μSR asymmetries versus time for $\text{YBa}_2(\text{Cu}_{0.96}\text{Ni}_{0.04})_3\text{O}_y$ ($y \sim 7$). The asymmetries are independent of temperature down to ~ 5 K. The change that occurs between 5 and 1.5 K (upper panel) is attributed to a change in the electron based magnetism. The strong dependence on applied longitudinal field (lower panel) points to the “quasi-static” nature of the electron based magnetism. The line adjustments are described in the text.

dipolar fields associated with electron based magnetic moments.

The asymmetries below ~ 5 K are not well described using the product of $P_Z^{\text{KT}}(t)$ and a simple exponential function $\exp(-\lambda_Z t)$. We found they are well accounted for either by taking the product with a stretched exponential $\exp[-(\lambda_Z t)^\beta]$ or by using a two component model:

$$a_s P_Z^s(t) = a_1 P_Z^{\text{KT}}(t) \exp(-\lambda_Z t) + a_2 P_Z^{\text{KT}}(t). \quad (3)$$

where the electron based magnetism influences the asymmetry in part of the sample (of relative volume a_1/a_s) and does not influence the asymmetry in the remaining part (of relative volume a_2/a_s). This component model is physically equivalent to the component model used to interpret the ^{170}Yb data (section III A).

With the stretched exponential model, we find that β remains below 1.0 and λ_Z increases with decreasing temperature. These results indicate a), there is a distribution in the spin-lattice fluctuation rates (which we relate to the distribution in the fluctuation rate of the magnetically correlated Cu(2) evidenced in section III A) and b),

the average electron based magnetic fluctuation rate decreases with decreasing temperature (as also evidenced in section III A).

With the two component model, at 3.0, 2.2, and 1.5 K respectively, we find a_1/a_s , the magnetic fraction, amounts to 0.28(16), 0.42(6) and 0.78(10) and λ_Z , the muon spin relaxation rate, amounts to $0.22(13) \times 10^6$, $0.52(9) \times 10^6$ and $1.29(5) \times 10^6 \text{ s}^{-1}$ respectively. According to this approach, as the temperature is progressively lowered a), an increasing fraction of the sample experiences electronic based magnetic fluctuations which have slowed down to enter the μSR frequency window and b), the average electron-based magnetic fluctuation rate decreases. We anticipate that μSR measurements at low enough temperatures below 1.5 K when analysed with the two component model will show that the asymmetries of all the muons are influenced by interactions with electron based magnetic moments.

The ^{170}Yb and μSR analyses thus lead to a common general description in terms of correlated Cu(2) magnetic moments with temperature dependent fluctuation rates. In addition, it seems likely that the approximate 30% volume fraction of the sample where the molecular field is “static” on the ^{170}Yb time-scale at 2.5 K, corresponds to the volume fraction ($\sim 28\%$ at 3.0 K, $\sim 42\%$ at 2.2 K) where μSR evidences electron-based magnetic moments. The observation that at temperatures just above 5 K, the fluctuations are too fast to be detected by μSR , whereas they are detected by ^{170}Yb indicates that the frequency window accessible for μSR is lower than that for ^{170}Yb .

To further examine the Cu(2) correlations, at 1.5 K we have measured the influence of applied longitudinal magnetic fields of 10 and 200 mT (Fig. 3). In these fields, the nuclear moments no longer influence the asymmetry. The strong dependence on applied field points to the “quasi-static” nature of the electron-based magnetic moments.

The fact that a field as small as $B_{\text{ext}} = 10 \text{ mT}$ has a strong influence on the asymmetry means that some of the correlations are characterised by a fluctuation rate smaller than $\gamma_\mu B_{\text{ext}} \simeq 10^7 \text{ s}^{-1}$ (the muon gyromagnetic ratio $\gamma_\mu = 851.615 \text{ Mrad s}^{-1} \text{ T}^{-1}$). These particular fluctuations are too slow to influence the ^{170}Yb lineshapes and they can be linked to the “static” subspectrum of Figs. 1 and 2. In fact, the form of the asymmetry with $B_{\text{ext}} = 10 \text{ mT}$ is relatively complex. At short times it is suggestive of an overdamped oscillation which would be indicative of correlations over lengths of a few lattice spacings¹⁸. However, because we know from the ^{170}Yb and the μSR measurements carried out in zero applied field that distributions exist in both the size and fluctuation rates of the correlated Cu(2) magnetic moments, it is not possible to carry out a productive quantitative analysis. This is also the case for the results obtained with $B_{\text{ext}} = 200 \text{ mT}$, where the asymmetry has an exponential form with $\lambda_Z = 0.021(1) \mu\text{s}^{-1}$ and where the whole asymmetry is accounted for.

μSR measurements have shown that when Ni is substituted into the different superconducting system

$\text{La}_{2-x}\text{Sr}_x\text{CuO}_4$, the dynamics of the Cu spin correlations which develop depend both on temperature (the fluctuation rates of the correlated Cu decrease with decreasing temperature) and on Ni content¹⁹.

IV. DISCUSSION

The ^{170}Yb Mössbauer and μSR analyses corroborate each other. Both analyses support the view that when the Cu in $\text{YBa}_2\text{Cu}_3\text{O}_y$ is substituted by 4% Ni, correlated and fluctuating Cu(2) magnetic moments (having a distribution in their size and in their fluctuation rate) are present over essentially all the whole sample volume. This suggests the length scale around a Ni over which the Cu(2) carry correlated magnetic moments is of the order of a few a/b lattice constants. The length scale around a Ni over which the Cu(2) carry staggered paramagnetic moments is similar¹⁰.

Since essentially all the Cu(2) carry correlated magnetic moments and the sample remains superconducting, the compound contains both localised holes (Cu(2) magnetic moments) and delocalised holes (which lead to superconductivity). We recall that we have no precise information concerning the size of the Cu(2) moments (section III A) and consequently the density of the localised holes is not known. In addition, it is difficult to assess the level of the superconducting condensate in the planes. Since the relation between T_{sc} and the condensate density may be non-linear in well doped samples²⁰, the fact that T_{sc} remains as high as 75 K does not automatically entail that the plane condensate density approaches that in unsubstituted optimally doped $\text{YBa}_2\text{Cu}_3\text{O}_7$. However, even though the condensate density in the chains may also contribute to maintaining superconductivity in the $\text{YBa}_2\text{Cu}_3\text{O}_y$ ²⁰, it seems very unlikely that T_{sc} could be as high as 75 K unless there is a significant contribution from a condensate density in the planes.

When substituted in $\text{YBa}_2\text{Cu}_3\text{O}_7$, Ni enters both the chain and plane sites with a significant fraction entering the plane site²¹. The structure remains orthorhombic and there is essentially no change in the oxygen level nor in the doping level^{9,22,23,24,25,26}. Penetration depth measurements, made down to 1.5 K, show that the superconducting condensate density increases progressively as the temperature is lowered²⁷. Above T_{sc} , the samples remain metallic and local spin susceptibility measurements²⁸ provide no evidence of a pseudogap. However, optical conductivity measurements indicates that a gap opens in the c-axis conductivity²⁴. The substitution of Ni also introduces paramagnetic moments which are compatible with effective spins of 1/2 to 1^{26,29}. In the sibling compound $\text{Bi}_2\text{Sr}_2\text{CaCu}_2\text{O}_{8+\delta}$, the substitution of Ni does not affect the superconducting gap³⁰.

Nuclear Quadrupole Resonance (NQR) measurements on superconducting $\text{YBa}_2\text{Cu}_3\text{O}_y$ substituted with Ni made above T_{sc} evidence that $1/T_1$, the nuclear spin relaxation rate, increases as the concentration of Ni

increases³¹. This indicates that the Cu(2) AF spin fluctuations that govern $1/T_1$ progressively change with Ni content.

Superconducting samples of $\text{YBa}_2(\text{Cu}_{1-x}\text{Ni}_x)_3\text{O}_y$ have been examined both above and below T_{sc} using NMR in 6 T on ^{17}O substituted in the Cu(2)-O planes^{9,10}. The observed hyperfine coupling is dominated by coupling to the spin polarisation of the two nearest in-plane Cu(2)^{32,33}. The measurements evidence a field induced staggered polarisation of the Cu(2) moments around each Ni and provide a direct static signature of the magnetic correlations within the Cu(2)-O planes. The ^{17}O probe is situated within a Cu(2)-O plane whereas the ^{170}Yb probe is situated between the two Cu(2)-O planes of a bilayer. With this probe, we evidence that Cu(2) magnetic correlations exist in absence of any applied field and they extend over the bilayers.

A possible mechanism through which substituted impurity spins may induce Cu(2) moments in the normal state of *underdoped* cuprates (spin-gap phase) has been examined theoretically within the t-J model treated with RVB mean-field theory³⁴. The sea of spinons which couple to the localised impurity spin is polarised by an external field and leads to a staggered Cu(2) spin polarisation. The polarisation decreases as r^{-3} with distance from the Ni impurity and the correlation length could be adjusted to reproduce the observed ^{17}O NMR line broadening⁹. This treatment pertains to underdoped cuprates where there is a pseudo-gap in the spin excitation spectrum. It does not appear to be relevant to the present case where there is no evidence of a pseudo-gap from local susceptibility measurements²⁸ (a gap is however evidenced in the c-axis conductivity²⁴) and where there is no applied magnetic field. Theoretical studies have also shown that d-wave superconductivity and antiferromagnetic order and π triplet pairs can exist near half filling³⁵. In addition, local antiferromagnetic order may appear near impurities and near some surfaces in a d-wave superconductor³⁶ and a phenomenological description based on Ginzburg-Landau theory, has suggested that induced antiferromagnetic moments may be nucleated in superconducting samples such that there are spatially varying order parameters³⁷. The appropriate theoretical description of the omnipresent nature of the correlated Cu(2) moments in well doped Ni substituted superconducting samples in zero applied field remains to be obtained.

To date, spontaneous correlated magnetic Cu(2) moments have been evidenced in fully oxidised superconducting samples of $\text{YBa}_2\text{Cu}_3\text{O}_7$ substituted with both Ni (this work) and with Co or Fe^{11,15}. Further information concerning the properties of magnetically correlated Cu(2) in Co substituted single crystals is given in

the following paper³⁸. Whereas each type of substitution (Ni or Co/Fe) lowers the superconducting transition temperature by approximately the same amount, each introduces quite different changes in some of the other properties. For example, Co enters only the Cu(1) site, the sample becomes underdoped and there is a pseudo-gap, seen for example in the local susceptibility²⁸. In contrast, Ni enters both the Cu(1) and the Cu(2) sites, the carrier density is not lowered and local susceptibility measurements show no evidence of a pseudo-gap²⁸. Consequently there is no univocal link between the appearance of magnetically correlated Cu(2) and the site occupied by the substituted cation nor with the fact that the substitution lowers or does not lower the doping level. There is no link either with the presence or absence of a spin susceptibility pseudo-gap.

We note that when a non-magnetic ion, for example Zn, is substituted into fully oxidised $\text{YBa}_2\text{Cu}_3\text{O}_7$, neither muon probe measurements³⁹ nor our ^{170}Yb measurements (made down to 1.4 K, unpublished) provide any evidence of magnetically correlated Cu(2) moments. NMR measurements do however evidence field induced paramagnetic moments¹⁰.

A straightforward feature thus appears to link the particular substituting cation and the correlated Cu(2) moments : these are observed when the substituting cation carries an intrinsic magnetic moment, irrespective both of the site it occupies and of the other changes it produces.

V. CONCLUSIONS

The present local probe measurements show that correlated Cu(2) magnetic moments are present over essentially all the sample volume of fully oxidised, optimally doped, superconducting $\text{YBa}_2(\text{Cu}_{0.96}\text{Ni}_{0.04})_3\text{O}_y$ ($y \sim 7$). The moments show distributions in their sizes and in their fluctuation rates which fall typically in the GHz range. The average fluctuation rate increases as the temperature increases. The Cu(2) moments, whose size, direction and correlation length remain to be established, coexist on an atomic level with high temperature superconductivity. The Cu(2)-O network of the planes is capable of supporting superconductivity when all the Cu(2) carry fluctuating correlated magnetic moments.

VI. ACKNOWLEDGEMENTS

J.A.H thanks Julien Bobroff for useful discussions and Nadine Genand-Riondet for assistance.

¹ Y. Sidis, C. Ulrich, P. Bourges, C. Bernhard, C. Niedermayer, L.P. Regnault, N.H. Andersen, B. Keimer Phys.

- ² B. Fauqué, Y. Sidis, V. Hinkov, S. Pailhès, C.T. Lin, X. Chaud, P. Bourges Phys. Rev. Lett. **96**, 197001 (2006)
- ³ G. J. MacDougall, A. A. Aczel, J. P. Carlo, T. Ito, J. Rodriguez, P. L. Russo, Y. J. Uemura, S. Wakimoto, G. M. Luke Phys. Rev. Lett. **101**, 017001 (2008)
- ⁴ J. Zaanen, O. Gunnarsson Phys. Rev. B **40**, 7391 (1989)
- ⁵ M. Kato, K. Machida, H. Nakanishi, M. Fujita J. Phys. Soc. Jap. **59**, 1047 (1990)
- ⁶ V.J. Emery, S.A. Kivelson, H.Q. Lin Phys. Rev. Lett. **64**, 475 (1990)
- ⁷ J.A. Hodges, P. Bonville, P. Imbert, G. Jéhanno, P. Debray Physica C **184**, 270 (1991)
- ⁸ S. Sachdev Rev. Mod. Phys. **75**, 913 (2003)
- ⁹ J. Bobroff, H. Alloul, Y. Yoshinari, A. Keren, P. Mendels, N. Blanchard, G. Collin, J.-F. Marucco Phys. Rev. Lett. **79**, 2117 (1997)
- ¹⁰ S. Ouazi, J. Bobroff, H. Alloul, M. Le Tacon, N. Blanchard, G. Collin, M.H. Julien, M. Horvatić, C. Berthier Phys. Rev. Lett. **96**, 127005 (2006)
- ¹¹ C. Vaast, J.A. Hodges, P. Bonville, A. Forget Phys. Rev. B **56**, 7886 (1997)
- ¹² J.A. Hodges, P. Bonville, P. Imbert, G. Jéhanno Physica C **184**, 259 (1991)
- ¹³ P. Dalmas de Réotier, A. Yaouanc J. Phys.: Condens. Matter **9**, 9113 (1997)
- ¹⁴ P. Dalmas de Réotier, P. C. M. Gubbens, A. Yaouanc J. Phys.: Condens. Matter **16**, S4687 (2004)
- ¹⁵ J.A. Hodges, Y. Sidis, P. Bourges, I. Mirebeau, M. Hennen, X. Chaud Phys. Rev. B **66**, 020501(R) (2002)
- ¹⁶ C. Bucci, R. De Renzi, G. Guidi, P. Carretta, F. Licci Nuovo Cimento D **16**, 1755 (1994)
- ¹⁷ N. Nishida, H. Miyatake, D. Shimada, S. Okuma, M. Ishikawa, T. Takabatake, Y. Nakazawa, Y. Kuno, R. Keitel, J.H. Brewer, T.M. Riseman, D. L. Williams, Y. Watanabe, T. Yamazaki, K. Nishiyama, K. Nagamine, E.J. Ansaldo, E. Torikai J. Phys. Soc. Japan **57**, 597 (1988)
- ¹⁸ A. Yaouanc, P. Dalmas de Réotier, Y. Chapuis, C. Marin, G. Lapertot, A. Cervellino, A. Amato Phys. Rev. B **77**, 092403 (2008)
- ¹⁹ T. Adachi, N. Oki, Risdiana, S. Yairi, Y. Koike Phys. Rev. B **78**, 134515 (2008)
- ²⁰ C. Bernhard, Ch. Niedermayer, U. Binninger, A. Hofer, Ch. Wenger, J. L. Tallon, G. V. M. Williams, E. J. Ansaldo, J. I. Budnick, C. E. Stronach, D. R. Noakes, M. A. Blankson-Mills Phys. Rev. B **52**, 10488 (1995)
- ²¹ S. Adachi, Y. Itoh, T. Machi, E. Kandyel, S. Tajima, N. Koshizuka Phys. Rev. B **61**, 4314 (2000)
- ²² J. Clayhold, N.P. Ong, Z.Z. Wang, J.M. Tarascon, P. Barbour Phys. Rev. B **39**, 7324 (1989)
- ²³ J. Clayhold, S.Hagen, Z.Z. Wang, N.P. Ong, J.M. Tarascon, P. Barbour Phys. Rev. B **39**, 777 (1989)
- ²⁴ A.V. Pimenov, A.V. Boris, Li Yu, V. Hinkov, Th. Wolf, J.L. Tallon, B. Keimer, C. Bernhard Phys. Rev. Lett. **94**, 227003 (2005)
- ²⁵ J.F. Bringley, T.M. Chen, B.A. Averill, K.M. Wong, S.J. Poon Phys. Rev. B **38**, 2432 (1988)
- ²⁶ K.A. Mirza, J.W. Loram, J.R. Cooper Physica C **235-240**, 1771 (1994)
- ²⁷ D.A. Bonn, S. Kamal, K. Zhang, R. Liang, D.J. Baar, E. Klein, W.N. Hardy Phys. Rev. B **50**, 4051, (1994)
- ²⁸ R. Dupree, A. Gencten, D. McK. Paul Physica C **193**, 81 (1992)
- ²⁹ P. Mendels, H. Alloul, G. Collin, N. Blanchard, J.F. Marucco, J. Bobroff Physica C **235-240**, 1595 (1994)
- ³⁰ E.W. Hudson, K.M. Lang, V. Madhavan, S.H. Pan, H. Eisaki, S. Uchida, J.C. Davis Nature (London) **411**, 920 (2001)
- ³¹ Y. Tokunaga, K. Ishida, Y. Kitaoka, K. Asayama Solid State Comm. **103**, 43 (1997)
- ³² Y. Yoshinari, H. Yasuoka, Y. Ueda, K. Koga, K. Kosuge J. Phys. Soc. Jpn. **59**, 3698 (1990)
- ³³ M. Takigawa, P. C. Hammel, R. H. Heffner, Z. Fisk, K. C. Ott, J. D. Thompson Phys. Rev. Lett. **63**, 1865 (1989)
- ³⁴ R. Kilian, S. Krivenko, G. Khaliullin, P. Fulde Phys. Rev. B **59**, 14432 (1999)
- ³⁵ M. Murakami, H. Fukuyama J. Phys. Soc. Japan **67** 41 (1998)
- ³⁶ Y. Ohashi Phys. Rev. B **60**, 15388 (1999)
- ³⁷ H. Kohno, H. Fukuyama, M. Sigrist J. Phys. Soc. Japan **68**, 1500 (1999)
- ³⁸ J.A. Hodges, P. Bonville, A. Yaouanc, P. Dalmas de Réotier, X. Chaud Phys. Rev. B **80**, 214505 (2009) (following paper)
- ³⁹ J.L. García-Muñoz, X. Obradors, S.H. Kilcoyne, R. Cywinski Physica C **185**, 1085 (1991)